IEICE TRANS. ELECTRON., VOL.E105–C, NO.8 AUGUST 2022

PAPER

Constant Voltage Design Using *K*-Inverter for Cooperative Inductive Power Transfer

Quoc-Trinh VO[†a)], ***Nonmember***, **Quang-Thang DUONG**[†b)], ***and*** **Minoru OKADA**[†c)], ***Members***

SUMMARY This paper proposes constant voltage design based on *K*-inverter for cooperative inductive power transfer (IPT) where a nearby receiver picks up power and simultaneously cooperates in relaying the signal toward another distant receiver. In a cooperative IPT system, wireless power is fundamentally transferred to the nearby receiver via one *K*-inverter and to the distant receiver via two *K*-inverters. By adding one more *K*-inverter to the nearby receiver, our design is among the simplest methods as it delivers constant output voltage to each receiver via two *K*-inverters only. Experimental results verify that the proposed cooperative IPT system can stabilize two output voltages against the load variations while attaining high RF-RF efficiency of 90%.

key words: *cooperative transmission, inductive power transmission, K-inverter, load-independent voltage*

1. Introduction

Inductive power transfer (IPT) [1] technology is undergoing a rapid development and attracting great attention from both academia and industry. IPT is a non-radiative type of energy transmission based on near-field coupling [2]. This technique has been applied in short-range applications, e.g., consumer electronics [3]–[6], implantable biomedical devices [7]–[10] and electric vehicles [11]–[14]. In such an application, the transmission distance is approximately less than or equal to the diameter of the coils. As the transmission distance surpasses this range, the coupling between the transmitter and receiver becomes very weak, such that the direct transmission cannot achieve a sufficient efficiency.

Relay transmission is an effective method to maintain a sufficient efficiency when the receiver is out of the direct transmission range [15], [16]. A relay coil will create an alternative transmission path consisting of two sufficiently strong couplings: transmitter-relay and relay-receiver. In the scenario where a transmitter is charging multiple receivers, there may be some receivers located in the vicinity of the transmitter while some others are located far from the transmitter. To improve the service quality for a far receiver, it would be better to have another receiver located in the middle of the path cooperate in the transmission, rather than placing a dedicated relay coil. Here, the nearby receiver has to play two roles: receiving power for its own load and relaying the signal toward the distant receiver. This scheme can be seen as cooperative IPT, in a manner analogous to cooperative transmission in wireless communications [17].

The concept of cooperative IPT has been first studied in [18], where each of the transmitter, the nearby receiver and the distant receiver was equipped with a series resonant coil. When the coils' reactances are canceled, an inductive coupling is equivalent to a *K*-inverter [19]. *K*-inverter is a popular two-port network which has been widely used for band-pass filter design [20], [21], load impedance transformation [22]–[24] and power division [25]. In addition to above mentioned characteristics, a *K*-inverter can output a load-independent current when driven by a constant voltage or a load-independent voltage when driven by a constant current. Accordingly, in the scheme of [18], the voltage source provided a constant current to the nearby receiver via one *K*-inverter and provided a constant voltage to the distant receiver via two consecutive *K*-inverters. As many applications (e.g., smartphone, camera) require steady voltage supplies for their efficient operations, it is necessary to design a compensation scheme for the cooperative IPT system so that it can deliver constant voltages to both the nearby and the distant receivers. Constant voltage design can help to isolate one receiver from the other and enable each receiver to independently control its received power by adjusting only its load resistance. Another important requirement for the design problem is to use circuit elements as few as possible to reduce copper loss.

Recently, several methods have been proposed to realize cooperative IPT systems with load-independent output voltages [26], [27]. For these methods, each of the transmitter and the distant receiver was equipped with one coil while the nearby receiver was equipped with two coils, namely the receiving coil and the transmitting coil. In [26], the series-parallel-series compensation scheme was used for each of the nearby receiver and the distant receiver while the series compensation was used for the transmitter. However, the design of the compensation scheme in [26] was based on the mutual inductance between two adjacent coils. Therefore, the stability of the load voltages over load variations would be sensitive to the misalignment of the coils. In contrast, the compensation scheme in [27] was designed regardless of the mutual inductance between the coils. For the method in [27], the distant receiver was compensated by series capacitor while each of the transmitter and the nearby receiver was compensated by the combination of series capacitor and

Manuscript received July 28, 2021.
Manuscript revised November 29, 2021.
Manuscript publicized January 31, 2022.

[†]The authors are with the Nara Institute of Science and Technology, Ikoma-shi, 630–0192 Japan.
a) E-mail: vo.quoc_trinh.vi3@is.naist.jp
b) E-mail: thang@is.naist.jp
c) E-mail: mokada@is.naist.jp

DOI: 10.1587/transele.2021ECP5038

capacitor-inductor-capacitor (CLC) topology. Accordingly, the load carried by the nearby receiver would consume a part of the power transferred from the source through two K-inverters formed by the CLC topology of the transmitter and by the coupling between the transmitter and the receiving coil of the nearby receiver. Then the rest of the power was continuously delivered to the load carried by the distant receiver through two other K-inverters formed by the CLC topology of the nearby receiver and by the coupling between the transmitting coil of the nearby receiver and the distant receiver. As a result, the load voltages were kept stable against the load variations because the loads carried by the nearby receiver and by the distant receiver were seen from the source via two K-inverters and four K-inverters respectively. However, the number of the circuit elements and the coils was not the least, leading to the increase of cooper loss.

In this paper, we propose a compensation scheme for cooperative IPT system to achieve load-independent output voltages while utilizing the least of circuit elements. Our proposal is an applicant of simultaneously charging two separate receivers where one receiver is inefficiently charged because of being located distant from the transmitter. In that scenario, other receiver can turn to cooperative mode to draw power for its load and help the distant receiver to be charged efficiently while still maintaining the isolation between two receivers. Novelties and contributions of this paper are as follows.

1. Our design implements a series resonant capacitor at the transmitter, a series resonant capacitor combined with a K-inverter at the nearby receiver and a series resonant capacitor at the distant receiver. This scheme is an extension of our previous works [28], [29] which limited the nearby receiver's compensation circuit to CLC topology only. In our scheme, the transmitter's voltage source delivers a constant voltage to each of the nearby receiver and the distant receiver via two K-inverters only. This is among the simplest structures to supply constant voltages to all the loads. Meanwhile, the method in [27] delivered constant voltages to the nearby receiver via two K-inverters and to the distant receiver via four K-inverters as mentioned above. Moreover, our previous evaluation [30] highlighted that our design using CLC topology could satisfy the requirement of constant load voltages while achieving higher transmission efficiency than the method in [27].
2. We provide K-inverter model based analysis and extensive experiments to evaluate the load voltage stability and RF-RF efficiency of the proposed design. Experimental results highlight that our scheme is able to stabilize the load voltages over a wide range of loads while attaining a high efficiency of up to 90%.

The rest of the paper is organized as follows. Section 2 describes the model of the conventional cooperative IPT system. Next, the proposed cooperative IPT system is illustrated in Sect. 3. Then, experimental results are shown in Sect. 4 to verify the theoretical analysis. Finally, Sect. 5 summarizes this paper.

2. System Model of Cooperative IPT System

Figure 1(a) in the next page illustrates the conventional cooperative IPT system including a transmitter (TX), a nearby receiver (RX_1) and a distant receiver (RX_2). The RX_1 is d_1 distant from the TX and d_2 distant from the RX_2. A power source generating a constant voltage V_0 is employed to drive the TX. It is assumed that the power source has negligibly small internal resistance. The power source operates at the angular frequency $\omega = 2\pi f$ where f is the operating frequency. Power is then delivered from the TX to the RX_1 through the mutual inductance M_{01} between them. The power received by the RX_1's coil is divided into two main parts. The first part of power is consumed by the load R_1 which the RX_1 carries. The second part of power is continuously delivered to the RX_2 through the mutual inductance M_{12} between the RX_1 and the RX_2. Then the power received by the RX_2's coil is consumed by the load R_2. It is noticed that the coupling M_{02} between the TX and the RX_2 is negligibly small because the cooperative IPT is employed only when the direct transmission is extremely weak.

In the conventional cooperative IPT system in Fig. 1(a), L_n and r_n denote the self-inductance and the internal resistance of the n-th coil respectively where $n \in \{0, 1, 2\}$. Each coil is compensated by a series resonant capacitor where

$$\omega = \frac{1}{\sqrt{L_0 C_0}} = \frac{1}{\sqrt{L_1 C_1}} = \frac{1}{\sqrt{L_2 C_2}}. \tag{1}$$

Basically, the coupling between two coils was modeled as a T-type CLC topology K-inverter in [19]. K-inverter is a famous two-port network which has been used to transform load impedance [22]–[24]. It means that if we terminate one port of an ideal K-inverter in an impedance Z, the other port will see a transformed impedance Z_{tf}

$$Z_{tf} = \frac{K^2}{Z}, \tag{2}$$

where K is the characteristic impedance of the K-inverter. Furthermore, if the internal resistances are small, a K-inverter outputs a load-independent current $I_{out} = -V_{in}/jK$ if driven by a voltage V_{in}, and it outputs a load-independent voltage $V_{out} = jKI_{in}$ if driven by a current I_{in}. As in Fig. 1(b), based on K-inverter model, the cooperative IPT system has three K-inverters corresponding to the mutual couplings among the coils. Specifically, the mutual coupling M_{01} is seen as the K-inverter K_{01} whose characteristic impedance $K_{01} = \omega M_{01}$. Similarly, the mutual couplings M_{12} and M_{02} are corresponding to the K-inverters K_{12} and K_{02} with the characteristic impedances $K_{12} = \omega M_{12}$ and $K_{02} = \omega M_{02}$ respectively. The corresponding values of the characteristic impedances of the K-inverters is shown in Table 1. Since the RX_2 is distant from the TX, the characteristic impedance K_{02} is relatively small to those of the

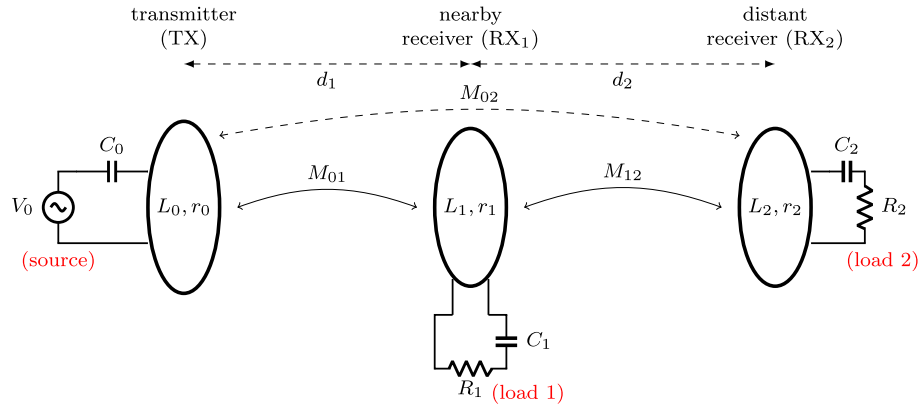

(a) System illustration

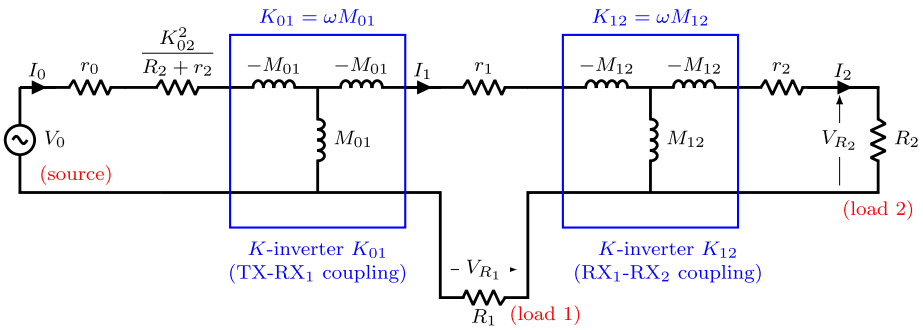

(b) K-inverter based model

Fig. 1 The conventional cooperative IPT system.

Table 1 K-inverters in the conventional cooperative IPT system and their characteristic impedances.

K-inverter's characteristic impedance	**Value**
K_{01}	ωM_{01}
K_{12}	ωM_{12}
K_{02}	ωM_{02}

K-inverters K_{01} and K_{12}. Therefore, power transferred from the TX to the two receivers via the K-inverters K_{01} and K_{12} is the most significant. For power transferred from the TX to the two receivers via the K-inverter K_{02}, only power transferred to the RX_2 is considered. Power transferred to the RX_1 via the K-inverters K_{02} and K_{12} is ignored because it is negligibly small to that transferred to RX_1 via the K-inverter K_{01}. As a consequence, the conventional cooperative IPT system can be modeled as in Fig. 1(b). (L_0, C_0), (L_1, C_1) and (L_2, C_2) are omitted in Fig. 1(b) for simplicity because each self-inductance is canceled out by corresponding capacitor. In Fig. 1(b), I_0, I_1 and I_2 are the currents flowing in the TX's coil, the RX_1's coil and the RX_2's coil respectively.

As shown in Fig. 1(b), the source V_0 sees the load R_1 via one K-inverter, leading that the current I_1 flowing in the nearby receiver's coil will be kept constant against the load variations. Therefore, the voltage across the load R_1 varies with the value of R_1. In contrast, the voltage across the load R_2 will be stabilized against the load variations because the source sees this load via two K-inverters. The K-inverter K_{12} yields a constant voltage V_{R_2} from constant current I_1. As a result, conventional cooperative IPT can provide constant voltage to only the distant receiver. The nearby receiver obtains a voltage varying with the load resistance. In practical applications, loads usually require constant voltages for their stable operations. Basically, to deliver constant source voltage to a load, the source needs to see that load via an even number of K-inverters. However, the number of K-inverters should be minimized to reduce the circuit elements and their associated copper loss.

3. The Proposed Cooperative IPT System

In order to deliver stable voltages to the two loads, we propose a cooperative IPT system using K-inverter as in Fig. 2(a). In comparison with the conventional cooperative IPT system, the RX_1 in the proposed system is additionally equipped a K-inverter to realize constant voltage characteristic against load variations for its load. In addition to being formed by inductive coupling, a K-inverter can be implemented using capacitors and inductors. Figure 3 is the description of K-inverters implemented by capacitors and inductors where the resonant relationship among the components inside the K-inverters at operating angular frequency ω is given

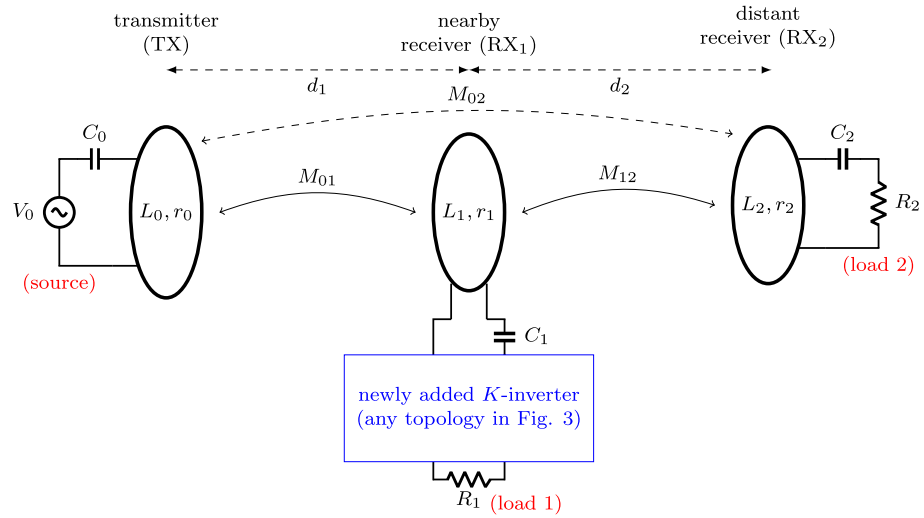

(a) System illustration

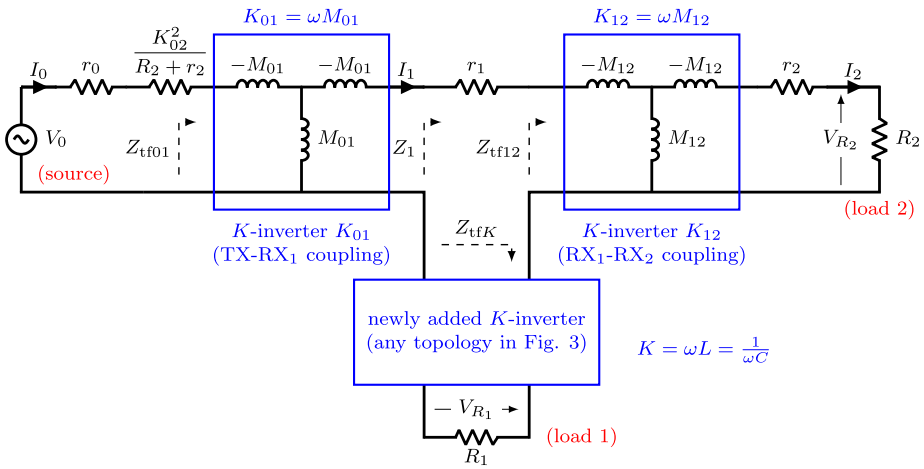

(b) K-inverter based model

Fig. 2 The proposed cooperative IPT system.

$$\omega = \frac{1}{\sqrt{LC}}. \tag{3}$$

Accordingly, the new K-inverter added to the RX_1 can be any topology as described in Fig. 3. The resonant relationship among the components of compensation circuits follows Eqs. (1) and (3). Based on K-inverter model, the proposed cooperative IPT system can be modeled as in Fig. 2(b) in the previous page. Similar to the conventional cooperative IPT system described above, in this model, K_{01}, K_{12} and K_{02} are the characteristic impedances of the K-inverters formed by the couplings M_{01}, M_{12} and M_{02} respectively while K is the characteristic impedance of the new K-inverter implemented at the RX_1. Table 2 shows the K-inverters in the proposed cooperative IPT system and their characteristic impedances. (L_0, C_0), (L_1, C_1) and (L_2, C_2) are omitted in Fig. 2(b) for simplicity because each self-inductance is canceled out by corresponding capacitor. Consequently, each of the loads in Fig. 2(b) is seen from the source via two K-inverters. Therefore, two load voltages will be stabilized

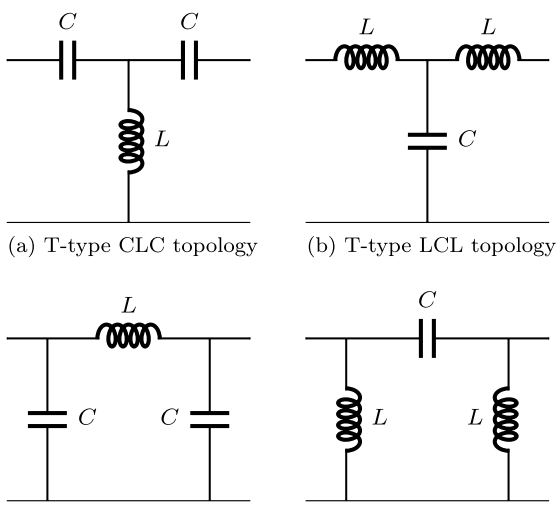

Fig. 3 Four implementations of K-inverter with characteristic impedance $K = \omega L = \frac{1}{\omega C}$.

Table 2 K-inverters in the proposed cooperative IPT system and their characteristic impedances.

K-inverter's characteristic impedance	Value
K_{01}	ωM_{01}
K_{12}	ωM_{12}
K_{02}	ωM_{02}
K	ωL or $\frac{1}{\omega C}$

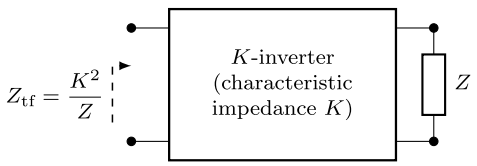

Fig. 4 Illustration of impedance transformation characteristic of a K-inverter used in IPT.

against the load variations. This structure is one of the simplest structures to realize the characteristics of cooperative transmission and constant load voltages in cooperative IPT systems. It can reduce the circuit elements and associated loss caused by their internal resistances.

The following analysis is based on the characteristic of impedance transformation of K-inverter which is illustrated in Fig. 4. The transformed impedance on the RX_1's coil from the total impedance of the distant receiver via the K-inverter K_{12}

$$Z_{\mathrm{tf12}} = \frac{K_{12}^2}{R_2 + r_2}. \tag{4}$$

Taking into account the transformation of the load R_1 via the K-inverter K, the impedance corresponding to the current flowing in the RX_1's coil is

$$Z_1 = r_1 + Z_{\mathrm{tf}K} + Z_{\mathrm{tf12}} = r_1 + \frac{K^2}{R_1} + \frac{K_{12}^2}{R_2 + r_2}. \tag{5}$$

Next, the impedance Z_1 is transformed by the K-inverter K_{01} to become Z_{tf01} on the TX's coil

$$Z_{\mathrm{tf01}} = \frac{K_{01}^2}{Z_1} = \frac{1}{\frac{1}{\frac{K_{01}^2}{K^2}R_1} + \frac{1}{\frac{K_{01}^2}{K_{12}^2}(R_2 + r_2)} + \frac{1}{\frac{K_{01}^2}{r_1}}}. \tag{6}$$

Then, the total impedance to the source V_0 is given by

$$\begin{aligned} Z_0 &= Z_{\mathrm{tf01}} + r_0 + \frac{K_{02}^2}{R_2 + r_2} \\ &= \frac{1}{\frac{1}{\frac{K_{01}^2}{K^2}R_1} + \frac{1}{\frac{K_{01}^2}{K_{12}^2}(R_2 + r_2)} + \frac{1}{\frac{K_{01}^2}{r_1}}} + \\ &\qquad r_0 + \frac{K_{02}^2}{R_2 + r_2}. \end{aligned} \tag{7}$$

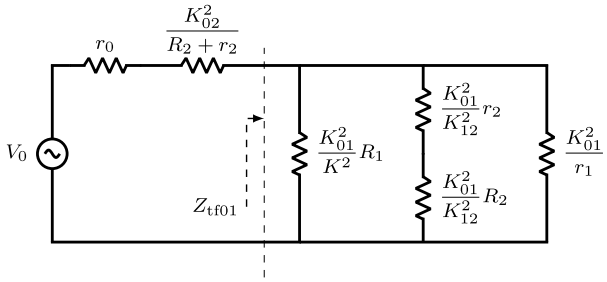

Fig. 5 The equivalent circuit of the proposed cooperative IPT system in Fig. 2(b).

Equation (7) shows that three terms, including $\frac{K_{01}^2}{K^2}R_1$, $\frac{K_{01}^2}{K_{12}^2}(R_2 + r_2)$ and $\frac{K_{01}^2}{r_1}$, are equivalently connected in parallel. Finally, all of them is connected in series to $\frac{K_{02}^2}{R_2+r_2}$ and r_0. Therefore, the equivalent circuit of the cooperative system is illustrated as in Fig. 5.

The voltage across the transformed impedance Z_{tf01} is

$$V_{\mathrm{tf01}} = \frac{Z_{\mathrm{tf01}}}{r_0 + \frac{K_{02}^2}{R_2 + r_2} + Z_{\mathrm{tf01}}} V_0. \tag{8}$$

The power consumed by R_1

$$\begin{aligned} P_{R_1} &= \frac{|V_{R_1}|^2}{R_1} = \frac{|V_{\mathrm{tf01}}|^2}{\frac{K_{01}^2}{K^2}R_1} \\ &= \frac{Z_{\mathrm{tf01}}^2}{\left(r_0 + \frac{K_{02}^2}{R_2 + r_2} + Z_{\mathrm{tf01}}\right)^2 \frac{K_{01}^2}{K^2}R_1}|V_0|^2 \\ &= \frac{K^2}{K_{01}^2}\frac{Z_{\mathrm{tf01}}^2}{\left(r_0 + \frac{K_{02}^2}{R_2 + r_2} + Z_{\mathrm{tf01}}\right)^2}\frac{|V_0|^2}{R_1}, \end{aligned} \tag{9}$$

where V_{R_1} is the voltage across the load R_1 and $|x|$ denotes the absolute value of the complex number x. The power consumed by R_2

$$\begin{aligned} P_{R_2} &= \frac{|V_{R_2}|^2}{R_2} \\ &= \frac{\left(\frac{R_2}{R_2 + r_2}\right)^2 |V_{\mathrm{tf01}}|^2}{\frac{K_{01}^2}{K_{12}^2}R_2} + \frac{R_2}{R_2 + r_2}\frac{K_{02}^2}{R_2 + r_2}|I_0|^2 \\ &= \frac{\left(\frac{R_2}{R_2 + r_2}\right)^2 |V_{\mathrm{tf01}}|^2}{\frac{K_{01}^2}{K_{12}^2}R_2} + \\ &\qquad \frac{R_2}{R_2 + r_2}\frac{K_{02}^2}{R_2 + r_2}\frac{|V_{\mathrm{tf01}}|^2}{Z_{\mathrm{tf01}}^2} \end{aligned}$$

$$= \frac{\dfrac{R_2}{(R_2+r_2)^2}}{\left(r_0 + \dfrac{K_{02}^2}{R_2+r_2} + Z_{\text{tf01}}\right)^2} \times \left(\frac{K_{12}^2}{K_{01}^2} Z_{\text{tf01}}^2 + K_{02}^2\right) |V_0|^2, \tag{11}$$

where V_{R_2} is the voltage across the load R_2.

From (9) and (11), the load voltages are derived

$$|V_{R_1}| = \frac{Z_{\text{tf01}}}{r_0 + \dfrac{K_{02}^2}{R_2+r_2} + Z_{\text{tf01}}} \frac{K}{K_{01}} |V_0|, \tag{12}$$

$$|V_{R_2}| = \frac{R_2}{R_2+r_2} \frac{\sqrt{\dfrac{K_{12}^2}{K_{01}^2} Z_{\text{tf01}}^2 + K_{02}^2}}{r_0 + \dfrac{K_{02}^2}{R_2+r_2} + Z_{\text{tf01}}} |V_0|. \tag{13}$$

Theoretically, the load voltages are not stable against the load variations because (12) and (13) contain the loads. Fortunately, in practice, the internal resistances are negligibly small to the loads

$$r_0 \ll Z_{\text{tf01}}, \tag{14}$$

$$r_2 \ll R_2. \tag{15}$$

When (14) and (15) hold, the mutual inductance M_{02} between the TX and the RX_2 is the key factor deteriorating the stability of the load voltages. However, as mentioned above that cooperative IPT is only employed as the mutual inductance M_{02} between the TX and the RX_2 is too weak. In the other words, the loads are often larger than the K-inverter impedance K_{02} in cooperative IPT systems

$$K_{02} \ll \frac{K_{12}}{K_{01}} Z_{\text{tf01}}, \tag{16}$$

$$K_{02}^2 \ll R_2 Z_{\text{tf01}}. \tag{17}$$

Therefore, the load voltages can be approximated as below

$$|V_{R_1}| \approx \frac{K}{K_{01}} |V_0| = \frac{L}{M_{01}} |V_0|, \tag{18}$$

$$|V_{R_2}| \approx \frac{K_{12}}{K_{01}} |V_0| = \frac{M_{12}}{M_{01}} |V_0|. \tag{19}$$

The above analysis illustrates the behaviors of the proposed cooperative IPT system as follows

- The load voltages are stabilized when the mutual inductance between the TX and the RX_2 is small. It is reasonable because the cooperative IPT is employed only when the TX is unable to deliver power to the RX_2 directly.
- The load voltages are only determined by the source voltage and the characteristic impedances of the K-inverters. This result confirms that each load is independently seen from the source via two K-inverters.
- Since the load voltages are irrelevant to the loads, the load voltages are expected to be stable against load variations under various coil arrangements.
- Based on the equivalent circuit of the whole system, the internal resistances of the TX's and RX_2's coils have a stronger effect on the load voltage stability than that of the RX_1's coil does. The internal resistance of the RX_1's coil causes the main energy loss in the system only.

4. Experimental Verification

4.1 Experiment Setup

The experiments are carried out to confirm the theoretical analysis. The experiment arrangement is illustrated in Fig. 6. In order to achieve high quality factor, the coils of the TX, the RX_1 and the RX_2 are made from litz wire 0.1mm × 100. Each coil is 15-turn coil with square shape and the size of 100mm × 100mm. The coils of the TX, the RX_1 and the RX_2 are coaxially arranged. In the experiments, the compensation networks for the TX, the RX_1 and the RX_2 are series, series combined with K-inverter and series as presented in the proposed cooperative IPT system in Sect. 3. Here, K-inverter is implemented using CLC topology in Fig. 3(a). Accordingly, the compensation circuit at the RX_1 is the combination of the series compensatory capacitor C_1 and T-type CLC topology. Therefore, C_1 and C are connected in series. For the sake of simplicity, an equivalent capacitor of the series combination of the series resonant capacitor C_1 for L_1 and capacitor C in additional K-inverter is built instead of constructing two separate capacitors. To create high-quality compensatory capacitors and inductor, each compensatory capacitor is implemented by combining several polyester film capacitors while the compensatory inductor in CLC topology is made from copper wire and a magnetic core. The loads R_1 and R_2 are the pure resistors. To investigate the load-independent characteristic of the load voltages of the proposed cooperative IPT system, the loads are changed different values in the set of {5Ω, 10Ω, 20Ω, 30Ω, 39Ω, 51Ω, 62Ω, 75Ω, 91Ω, 100Ω}.

An DC power source of 10V is used to supply for the inverter PATO23-1. The inverter is tuned to generate the signal with the frequency of 200kHz. However, since the output waveform of the inverter is unstable against its load, a filter is utilized to create a stable signal with the frequency

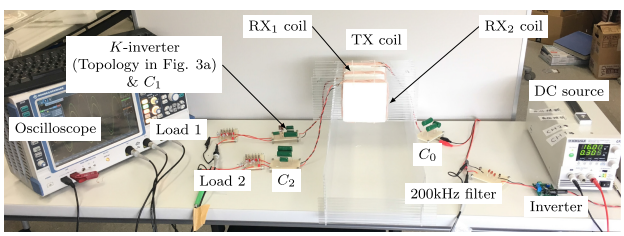

Fig. 6 Experiment arrangement of the cooperative IPT system.

Table 3 List of practical parameter values

Symbol	Parameter	Value
L_0	self-inductance of TX coil	51.56μH
r_0	internal resistance of TX coil	0.312Ω
C_0	resonant capacitor for L_0	12.38nF
L_1	self-inductance of RX_1 coil	50.96μH
r_1	internal resistance of RX_1 coil	0.312Ω
C_1 and C in series	equivalent capacitor of series combination of resonant capacitor C_1 for L_1 and capacitor C in K-inverter K	11.3nF
L	inductor in K-inverter K	6.35μH
C	capacitor in K-inverter K	99.6nF
L_2	self-inductance of RX_2 coil	50.8μH
r_2	internal resistance of RX_2 coil	0.284Ω
C_2	resonant capacitor for L_2	12.56nF

Table 4 List of the measured characteristic impedances of the K-inverters in initial coil arrangement (d_1 = 60mm, d_2 = 60mm)

Symbol	Parameter	Value
K_{01} (ωM_{01})	characteristic impedance of the K-inverter formed by the coupling between TX's coil and RX_1's coil	7.97Ω
K_{12} (ωM_{12})	characteristic impedance of the K-inverter formed by the coupling between RX_1's coil and RX_2's coil	7.95Ω
K_{02} (ωM_{02})	characteristic impedance of the K-inverter formed by the coupling between TX's coil and RX_2's coil	2.64Ω
K (ωL)	characteristic impedance of the K-inverter formed by additional CLC topology	7.98Ω

of 200kHz. Then the output signal of the filter is considered as the input voltage of the cooperative IPT system. Consequently, the load voltages and the RF-RF efficiency in the following experiments will be observed based on the output signal of the filter. In our experiments, the oscilloscope RTO 1004 is employed to measure the voltages. The values of the system's components after constructed are measured by LCR meter. Their values are listed as in Table 3.

4.2 RF Power Calculation

In order to evaluate the RF-RF efficiency, the input power is calculated based on the input voltage and the input current. In our calculation, the input current is indirectly measured using the voltage across and the current flowing through the compensatory capacitor C_0 of the TX's coil. It is paid attention that the compensatory capacitor C_0 is the high quality one, therefore it is considered that its internal resistance contributes negligibly small effect on phase difference between its voltage and its current. Consequently, the current flowing in the capacitor C_0 leads the voltage across itself by nearly 90^0. Accordingly, the process to estimate the input current is described as below

- V_{C_0} is shifted back to 90^0
- Then, the shifted V_{C_0} is divided by $1/(\omega C_0)$ to estimate the input current

For example, Fig. 8 illustrates the estimate of the input current of the cooperative IPT system when the loads are equal to 100Ω and the distances d_1 and d_2 are equal to 60mm.

Finally, from the estimated input current I_0 and the measured input voltage V_0, the RF input power is estimated

$$P_{\text{in (RF)}} = \frac{1}{M}\sum_{m=1}^{M} V_0[m]I_0[m] \tag{20}$$

where M is the number of the samples over one period of the signal while $V_0[m]$ and $I_0[m]$ are the values of the input voltage and the estimated current flowing through the source of the m-th sample in the period of the signal.

Similarly, the output power is estimated through the measured load voltages as follows

$$P_{\text{out (RF)}} = \frac{1}{M}\sum_{m=1}^{M}\left(\frac{V_{R_1}^2[m]}{R_1} + \frac{V_{R_2}^2[m]}{R_2}\right) \tag{21}$$

where $V_{R_1}[m]$ and $V_{R_2}[m]$ are the load voltages of the m-th sample in the period of the signal.

Then the RF-RF efficiency is calculated by the formula $\eta = P_{\text{out (RF)}}/P_{\text{in (RF)}}$.

4.3 Performance in Initial Coil Arrangement

Initially, the distance between any two adjacent coils is 60mm ($d_1 = d_2 = 60$mm). In this arrangement, both load voltages are designed to be equal to the source voltage. Therefore, the new K-inverter K added at the RX_1 is designed so that its characteristic impedance is equal to the characteristic impedance of the K-inverter K_{01}. It leads to $\omega L = \frac{1}{\omega C} = \omega M_{01}$. The measured characteristic impedances of the K-inverters are given in Table 4. Accordingly, the ratios between each load voltage and the source voltage as in Eqs. (18) and (19) are calculated about 1.

Figure 9 shows the ratios between the load voltages and the input voltage over the load variations. In these results, when the loads vary from 5Ω to 100Ω the voltage ratio $|V_{R_1}|/|V_{\text{in}}|$ varies from about 0.8 to nearly 1 and the voltage ratio $|V_{R_2}|/|V_{\text{in}}|$ varies from about 0.7 to around 0.95 respectively. The results indicate that when the loads become larger than 10Ω, the voltage ratios approach the stable values. This agrees with the estimates in (18)-(19). For the range of small loads, from 5Ω to 10Ω, the load volt-

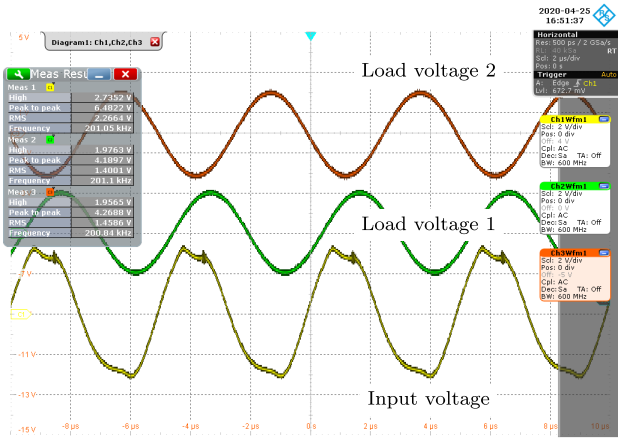

Fig. 7 Signal waveform of the load voltages and the input voltages when the loads are approximately equal to 5Ω and the distances $d_1 = d_2 = 60$mm.

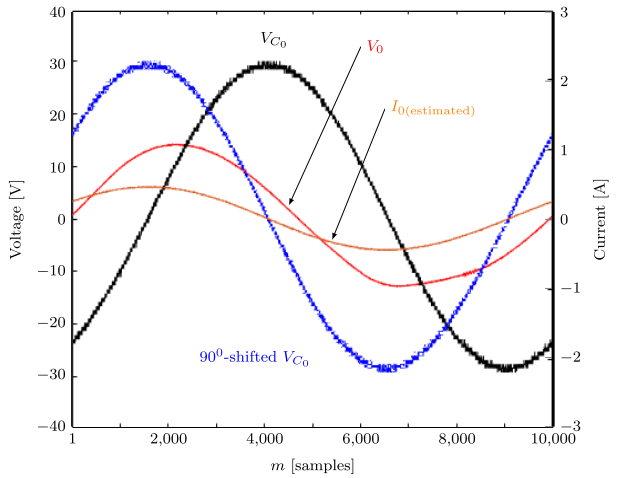

Fig. 8 The 1-period waveform of the input voltage and of the estimated input current when the loads are equal to 100Ω.

ages are slightly far away from the stable values because the mutual coupling between the TX and the RX_2 is relatively large to the loads. Figure 7 is a snapshot of the measured voltages when the loads are equal to 5Ω and the distances $d_1 = 60$mm, $d_2 = 60$mm. Statistically, the means of the measures of the load voltages V_{R_1} and V_{R_2} are 0.94 and 0.89 of the input voltage respectively. The corresponding corrected sample standard deviations [32] of the measures of two load voltages V_{R_1} and V_{R_2} are about 6.2% and 8.2% in comparison with the mean values. These values are less than 10%, meaning that the load voltages are considered as being stable against the load variations. On the other hand, the results also confirm the cooperative characteristic of the nearby receiver, which is to support the transmitter to deliver power to a distant receiver and draw power for its load.

Figure 10 has plotted the graph of RF-RF efficiency of the cooperative IPT system over the load variations. In general, the results highlight that the cooperative IPT system achieves high RF-RF efficiency of between 78% and 90% when the loads vary from 5Ω to 100Ω. When the loads in-

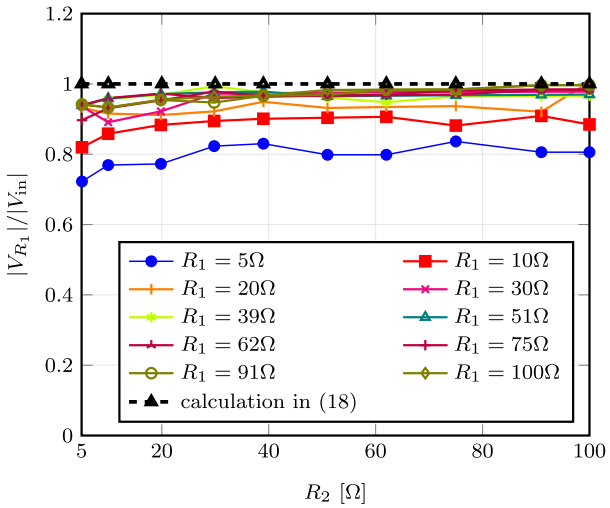

(a)

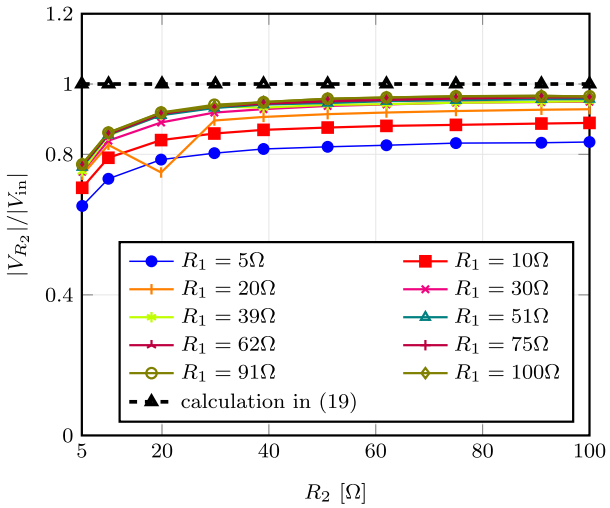

(b)

Fig. 9 The voltage ratio between the load voltages and the input voltage over the load variations for the case $d_1 = 60$mm, $d_2 = 60$mm

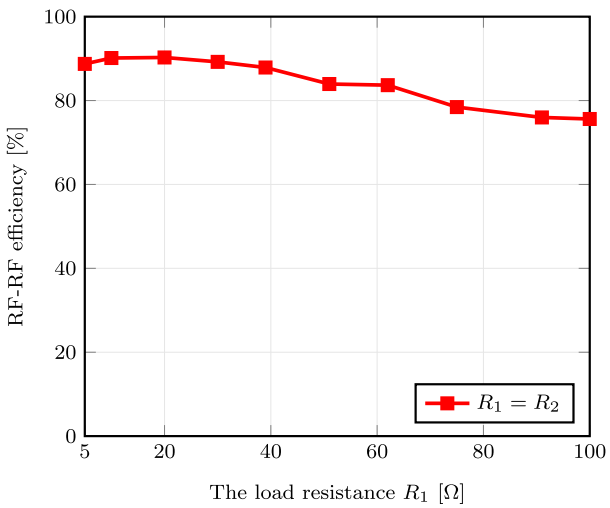

Fig. 10 The RF-RF efficiency as a function of the loads for the case $d_1 = d_2 = 60$mm ($R_1 = R_2$)

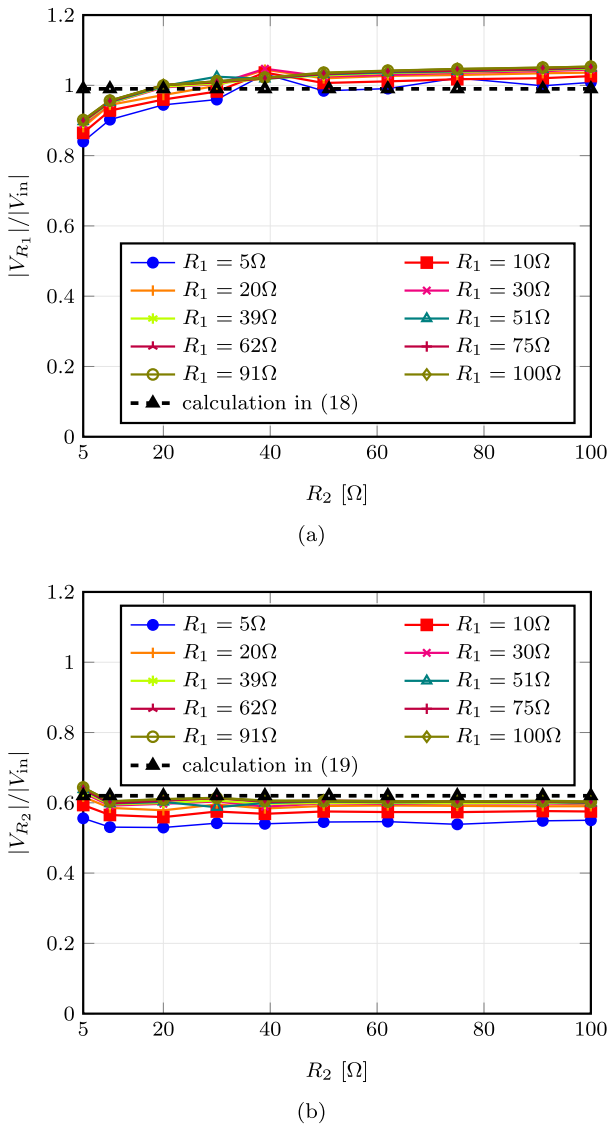

Fig. 11 The voltage ratio between the load voltages and the input voltage over the load variations for the case $d_1 = 60\text{mm}, d_2 = 80\text{mm}$.

crease from 5Ω to 40Ω the proposed cooperative IPT system attains the RF-RF efficiency of about 90%. Then, the efficiency gradually decreases from 90% to 78% when the loads increase from 40Ω to 100Ω.

4.4 Performance in Other Coil Arrangements

In this section, we investigate the load voltage stability and the RF-RF efficiency of the cooperative system for several coil arrangements. All circuit parameters are kept unchanged as in initial design when investigating the performance of the proposed cooperative IPT system under different coil arrangements. Figure 11 in the next page is the experimental results of the load voltages over the load variations when the distance d_2 increases to 80mm. For this arrangement, the measured characteristic impedances of the K-inverters are listed in Table 5. Accordingly, the estimated

Table 5 List of the measured characteristic impedances of the K-inverters in misalignment ($d_1 = 60\text{mm}, d_2 = 80\text{mm}$)

Symbol	Parameter	Value
K_{01} (ωM_{01})	characteristic impedance of the K-inverter formed by the coupling between TX's coil and RX_1's coil	8.06Ω
K_{12} (ωM_{12})	characteristic impedance of the K-inverter formed by the coupling between RX_1's coil and RX_2's coil	4.99Ω
K_{02} (ωM_{02})	characteristic impedance of the K-inverter formed by the coupling between TX's coil and RX_2's coil	1.65Ω
K (ωL)	characteristic impedance of the K-inverter formed by additional CLC topology	7.98Ω

ratios between each load voltage and the source voltage using Eqs. (18) and (19) are 0.99 and 0.62.

The results indicate that when the loads vary from 5Ω to 20Ω the ratio between the load voltage V_{R_1} and the input voltage increases from around 0.85 to nearly 1. Then it is stable at this ratio against the increase of the loads. This ratio is similar to that in the initial design. It agrees with the estimate in (18) since there is no change of the characteristic impedances of the K-inverters K_{01} and K. Meanwhile, the ratio between the load voltage V_{R_1} and the input voltage is kept stable at around 0.59 when the loads increase from 5Ω to 100Ω. The ratio between the load voltage V_{R_1} and the input voltage decrease in comparison with the initial design because the characteristic impedance of the K-inverter K_{12} decreases while that of the K-inverter K_{01} is fixed. Again, the experimental results confirms the estimate of the load voltage V_{R_2} in (19). Moreover, the distance between the TX and the RX_2 is longer, leading to the decrease of the coupling between them. Accordingly, the load voltages in this setting are easier to approach the stable values than those in the initial setting. The measures of the ratios $|V_{R_1}|/|V_{\text{in}}|$ and $|V_{R_2}|/|V_{\text{in}}|$ have the mean values of 1 and 0.595 respectively. The standard deviations of the measures are 0.05 and 0.023. They are only equal 5.04% and 3.87% of the corresponding mean values. It means that the load voltages still stable against the load variations for the coil arrangement with $d_1 = 60\text{mm}$ and $d_2 = 80\text{mm}$.

Figure 12 illustrates the RF-RF efficiency of the proposed cooperative IPT system under four cases of coil arrangements: ($d_1 = 60\text{mm}, d_2 = 80\text{mm}$), ($d_1 = 60\text{mm}, d_2 = 40\text{mm}$), ($d_1 = 40\text{mm}, d_2 = 60\text{mm}$), ($d_1 = 80\text{mm}, d_2 = 60\text{mm}$). Under various coil arrangements, the proposed cooperative IPT system attains the RF-RF efficiency of from 80% to over 90% when the loads vary from 10Ω to 50Ω. The RF-RF efficiency gradually decreases as the loads increase over 50Ω. Although the loads are equal to 90Ω, the

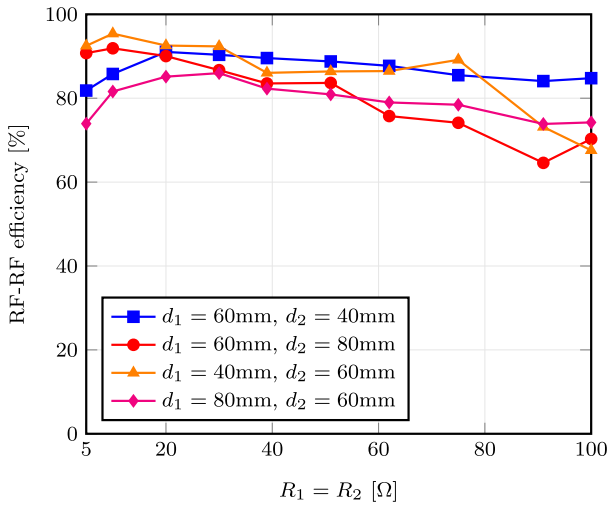

Fig. 12 The RF-RF efficiency as a function of the loads under four coil arrangements

lowest RF-RF efficiency of over 60% is achieved for the case of ($d_1 = 60$mm, $d_2 = 80$mm) while the proposed IPT system can achieve the RF-RF efficiency of from 70% to nearly 90% for other cases of coil arrangements.

5. Conclusion

This paper utilized K-inverter to propose the cooperative IPT system where the nearby receiver could simultaneously draw power for its load and relay the received power to the distant receiver. Although K-inverter was a two-port device which was initially designed as a microwave filter, it has been then exploited as a resonant compensation circuit with the characteristic of impedance transformation in IPT systems. By adding only one K-inverter to the nearby receiver, we realized one of the simplest structures for cooperative IPT systems to stabilize the load voltages against load variations as each of the loads was seen from the source via two K-inverters. The load voltages were then decided by the characteristic impedances of the K-inverters and the source voltage only. The experiments were carried out to verify the theoretical analysis of the load voltage stability and to evaluate the RF-RF efficiency of the cooperative IPT system. For the performance in the initial coil arrangement, the proposed cooperative IPT system could deliver the stable voltages to the loads with the corresponding corrected sample standard deviations of under 10% of the mean values. Meanwhile, the highest RF-RF efficiency that the cooperative IPT system could achieve was about 90% which was acceptable for many inductive power transfer systems. In the other coil arrangements, two load voltages were still stable against load variations while the RF-RF efficiency of over 80% was achieved when the loads varied from 10Ω to 50Ω.

Acknowledgments

This work was supported by JSPS KAKENHI Grant Number 20K14736.

References

[1] G.A. Covic and J.T. Boys, "Inductive power transfer," Proc. IEEE, vol.101, no.6, pp.1276–1289, June 2013.
[2] Z. Zhang, H. Pang, A. Georgiadis, and C. Cecati, "Wireless power transfer-an overview," IEEE Trans. Ind. Electron., vol.66, no.2, pp.1044–1058, Feb. 2019.
[3] J.A. Taylor, Z.N. Low, J. Casanova, and J. Lin, "A wireless power station for laptop computers," 2010 IEEE Radio and Wireless Symp. (RWS), IEEE, Jan. 2010.
[4] J. Kim, H.-C. Son, D.H. Kim, and Y.J. Park, "Optimal design of a wireless power transfer system with multiple self-resonators for an LED TV," IEEE Trans. Consum. Electron., vol.58, no.3, pp.775–780, Aug. 2012.
[5] S.Y. Hui, "Planar wireless charging technology for portable electronic products and Qi," Proc. IEEE, vol.101, no.6, pp.1290–1301, June 2013.
[6] P.S. Riehl, A. Satyamoorthy, H. Akram, Y.C. Yen, J.C. Yang, B. Juan, C.M. Lee, F.C. Lin, V. Muratov, W. Plumb, and P.F. Tustin, "Wireless power systems for mobile devices supporting inductive and resonant operating modes," IEEE Trans. Microw. Theory Techn., vol.63, no.3, pp.780–790, March 2015.
[7] A. Yakovlev, S. Kim, and A. Poon, "Implantable biomedical devices: Wireless powering and communication," IEEE Commun. Mag., vol.50, no.4, pp.152–159, April 2012.
[8] B.H. Waters, A.P. Sample, P. Bonde, and J.R. Smith, "Powering a ventricular assist device (VAD) with the free-range resonant electrical energy delivery (FREE-d) system," Proc. IEEE, vol.100, no.1, pp.138–149, Jan. 2012.
[9] H.Y. Leung, D. McCormick, D. Budgett, and A.P. Hu, "Design methodology for inductive power transfer systems targeting high power implantable devices," 2013 IEEE Int. Symp. on Circuits and Syst. (ISCAS2013), IEEE, May 2013.
[10] D. Ahn and S. Hong, "Wireless power transmission with self-regulated output voltage for biomedical implant," IEEE Trans. Ind. Electron., vol.61, no.5, pp.2225–2235, May 2014.
[11] Z. Zhang and K.T. Chau, "Homogeneous wireless power transfer for move-and-charge," IEEE Trans. Power Electron., vol.30, no.11, pp.6213–6220, Nov. 2015.
[12] R. Bosshard and J.W. Kolar, "Multi-objective optimization of 50 kW/85 kHz IPT system for public transport," IEEE J. Emerg. and Sel. Topics in Power Electron., vol.4, no.4, pp.1370–1382, Dec. 2016.
[13] Y.J. Jang, "Survey of the operation and system study on wireless charging electric vehicle systems," Transportation Research Part C: Emerg. Technol., vol.95, pp.844–866, Oct. 2018.
[14] A. Ramezani, S. Farhangi, H. Iman-Eini, B. Farhangi, R. Rahimi, and G.R. Moradi, "Optimized LCC-series compensated resonant network for stationary wireless EV chargers," IEEE Trans. Ind. Electron., vol.66, no.4, pp.2756–2765, April 2019.
[15] A. Kurs, A. Karalis, R. Moffatt, J.D. Joannopoulos, P. Fisher, and M. Soljačić, "Wireless power transfer via strongly coupled magnetic resonances," Science, vol.317, no.5834, pp.83–86, July 2007.
[16] Y. Ota, T. Takura, F. Sato, and H. Matsuki, "Wireless power transfer by low coupling electromagnetic induction - LC booster," 2012 IEEE MTT-S Int. Microw. Workshop Series Innovative Wireless Power Transmission: Technol., Syst., and Appl., IEEE, May 2012.
[17] A. Nosratinia, T. Hunter, and A. Hedayat, "Cooperative communication in wireless networks," IEEE Commun. Mag., vol.42, no.10, pp.74–80, Oct. 2004.
[18] Y. Zhang, T. Lu, Z. Zhao, K. Chen, F. He, and L. Yuan, "Wireless power transfer to multiple loads over various distances using relay resonators," IEEE Microw. Wireless Compon. Lett., vol.25, no.5, pp.337–339, May 2015.
[19] J. Kuang, B. Luo, Y. Zhang, Y. Hu, and Y. Wu, "Load-isolation wireless power transfer with k-inverter for multiple-receiver appli-

cations," IEEE Access, vol.6, pp.31996–32004, April 2018.
[20] I. Awai, "Design theory of wireless power transfer system based on magnetically coupled resonators," 2010 IEEE Int. Conf. Wireless Inf. Technol. and Syst., IEEE, Aug. 2010.
[21] I. Awai, "BPF theory-based design method for wireless power transfer system by use of magnetically coupled resonators," IEEJ Trans. Electron., Inf. and Syst., vol.130, no.12, pp.2192–2197, 2010.
[22] J.S. Hong, Microstrip Filters for RF/Microwave Applications, 2 ed., ch. 3, pp.54–62, John Wiley & Sons, 2011.
[23] B. Luo, S. Wu, and N. Zhou, "Flexible design method for multi-repeater wireless power transfer system based on coupled resonator bandpass filter model," IEEE Trans. Circuits and Syst. I: Regular Papers, vol.61, no.11, pp.3288–3297, Nov. 2014.
[24] J. Zhou, B. Luo, X. Zhang, and Y. Hu, "Extendible load-isolation wireless charging platform for multi-receiver applications," IET Power Electron., vol.10, no.1, pp.134–142, Jan. 2017.
[25] K.E. Koh, T.C. Beh, T. Imura, and Y. Hori, "Impedance matching and power division using impedance inverter for wireless power transfer via magnetic resonant coupling," IEEE Trans. Ind. Appl., vol.50, no.3, pp.2061–2070, May 2014.
[26] C. Cheng, Z. Zhou, W. Li, J. Lu, Z. Deng, and C.C. Mi, "Long-distance wireless power transfer system powering multiple loads with constant voltage outputs using S-SP compensation," IET Power Electron., vol.13, no.9, pp.1729–1734, July 2020.
[27] C. Cheng, W. Li, Z. Zhou, Z. Deng, and C. Mi, "A load-independent wireless power transfer system with multiple constant voltage outputs," IEEE Trans. Power Electron., vol.35, no.4, pp.3328–3331, April 2020.
[28] Q.T. Vo, Q.T. Duong, and M. Okada, "Cooperative transmission in three-coil inductive power transfer system with load-independent output voltages," 2019 Int. Workshop on Antenna Technol. (iWAT), IEEE, Florida, USA, March 2019.
[29] Q.T. Vo, Q.T. Duong, and M. Okada, "Efficiency improvement for three-coil cooperative inductive power transfer systems," 2019 IEEE Wireless Power Transfer Conf. (WPTC), IEEE, London, UK, June 2019.
[30] Q.T. Vo, Q.T. Duong, and M. Okada, "Efficiency comparison of cooperative inductive power transfer systems," 2020 Int. Conf. Advanced Technol. for Commun. (ATC), IEEE, Nha Trang, Viet Nam, Oct. 2020.
[31] T. Imura and Y. Hori, "Maximizing air gap and efficiency of magnetic resonant coupling for wireless power transfer using equivalent circuit and neumann formula," IEEE Trans. Ind. Electron., vol.58, no.10, pp.4746–4752, Oct. 2011.
[32] M. Hardy, "An illuminating counterexample," Amer. Math. Monthly, vol.110, no.3, pp.234–238, March 2003.

Quoc-Trinh Vo received the B.E. degree in electronics-telecommunications engineering from Da Nang University of Science and Technology, Viet Nam, in 2010, the M.E in electronics engineering from International University, Vietnam National University, Ho Chi Minh City, Viet Nam, in 2013, and the D.Eng. from Nara Institute of Science and Technology, Nara, Japan, in 2021. He is currently postdoc researcher in Nara Institute of Science and Technology, Nara, Japan. His interests include wireless power transfer, wireless communication and digital signal processing.

Quang-Thang Duong received the B.E., M.E., and Ph.D. degrees in communications engineering from Osaka University, Osaka, Japan, in 2009, 2011, and 2014, respectively. He is currently an Assistant Professor with the Nara Institute of Science and Technology, Nara, Japan. His current research interests include broadband wireless access techniques, channel estimation, information theories, error correcting codes, wireless power transfer, and simultaneous wireless information, and power transfer.

Minoru Okada received the B.E. degree in communications engineering from the University of Electro-Communications, Tokyo, Japan, in 1990, and the M.E. and Ph.D. degrees in communications engineering from Osaka University, Osaka, Japan, in 1992 and 1998, respectively. From 1993 to 2000, he was a Research Associate with Osaka University. From 1999 to 2000, he was a Visiting Research Fellow with the University of Southampton, Southampton, U.K. In 2000, he joined the Graduate School of Information Science, Nara Institute of Science and Technology, Ikoma, Japan, as an Associate Professor and then became a Professor. His current research interests include wireless communications, including WLAN, WiMAX, code division multiple access, OFDM, and satellite communications. Dr. Okada is a member of the Institute of Television Engineers of Japan, Institute of Electrical, Information, and Communication Engineers (IEICE), Japan, and the Information Processing Society Japan. He was the recipient of the Young Engineer Award from the IEICE in 1999.